Linking Experimental and Ab-initio Thermochemistry of Adsorbates with a Generalized Thermochemical Hierarchy

Bjarne Kreitz,* Kento Abeywardane, and C. Franklin Goldsmith*

School of Engineering, Brown University, Providence, RI 02912, United States

E-mail: bjarne_kreitz@brown.edu; franklin_goldsmith@brown.edu

Abstract

Enthalpies of formation of adsorbates are crucial parameters in the microkinetic modeling of heterogeneously catalyzed reactions, since they quantify the stability of intermediates on the catalyst surface. This quantity is often computed using density functional theory, as more accurate methods are computationally still too expensive, which means that derived enthalpies have a large uncertainty. In this study, we propose a new error cancellation method to compute the enthalpies of formation of adsorbates more accurately from DFT through a generalized connectivity-based hierarchy. The enthalpy of formation is determined through a hypothetical reaction that preserves atomistic and bonding environments. The method is applied to a dataset of 60 adsorbates on Pt(111) with up to 4 heavy (non-hydrogen) atoms. Enthalpies of formation of the fragments required for the bond balancing reactions are based on experimental heats of adsorption for Pt(111). Thus, the proposed methodology creates an interconnected thermochemical network of adsorbates that combines experimental with *ab-initio* thermochemistry in a single thermophysical database.

Introduction

Activity and selectivity of a catalytic material are governed on the atomistic scale by the free energy landscape, which is shaped by the stability of adsorbed intermediates and transition states. Accordingly, accurate parameterization of the thermophysical properties of the adsorbed intermediates – primarily enthalpy and entropy – is of paramount importance in elucidating the mechanism and microkinetic modeling.[1–4] The entropy of an adsorbate is a species-specific quantity that can be determined by the partition function using the harmonic oscillator model, or with more accurate methods that include anharmonic effects.[5,6] In contrast, the enthalpy of an adsorbate is not just a result of the partition function. As an energy, it only has a physical meaning relative to some reference state. Although the choice of reference energy is arbitrary, some reference states are more convenient than others. Perhaps the most common and convenient choice is the enthalpy of formation, $\Delta_\mathrm{f}H$ (often referred to as the "heat of formation"). When referenced to the same reference state, the set of all chemical species, both gas phase and adsorbed, form a thermochemical network (TN).

Although experimentally determined enthalpies of formation may be preferred, the enthalpies of formation for the vast majority of the species in large gas-phase kinetic mechanisms (*e.g.* combustion and atmospheric chemistry) have never been measured and are unlikely ever to be measured (particularly open-shell species). In heterogeneous catalysis, the situation is arguably much worse. Only a few experimentally collected enthalpies of formation of adsorbates are available from carefully conducted single crystal adsorption calorimetry or temperature-programmed desorption.[7–9] In all of these cases, the missing values must either be estimated (*e.g.* via group additivity[10–12]), or computed from quantum-mechanical (QM) calculations.[13] In the latter case, the standard approach is to formulate a hypothetical reaction in which the target species, P (for which $\Delta_\mathrm{f}H$ is unknown), is formed from reactants (for which the $\Delta_\mathrm{f}H$ are known): *e.g.* aA + bB + cC $\longrightarrow$ P. The reaction enthalpy at 0 K, $\Delta H^\mathrm{QM}_\mathrm{rxn}$, is computed using an electronic structure method

$$\Delta H^\mathrm{QM}_\mathrm{rxn} = E^\mathrm{P}_0 + \sum_{i\neq\mathrm{P}} \nu_i E^i_0 \tag{1}$$

where E^i_0 is the sum of electronic and zero-point energy for species i obtained by the QM calculations, and ν_i is the stoichiometric coefficient. The enthalpy of formation of P at 0 K is then given by

$$\Delta_\mathrm{f}H^\mathrm{P}\,(0\mathrm{K}) = \Delta H^\mathrm{QM}_\mathrm{rxn} - \sum_{i\neq\mathrm{P}} \nu_i \Delta_\mathrm{f}H^i\,(0\mathrm{K}) \tag{2}$$

The accuracy of $\Delta_\mathrm{f}H^\mathrm{P}$ (we drop the temperature for simplicity) depends upon the uncertainty of the two terms on the right-hand side of Equation (2). With the development of the Active

Thermochemical Tables (ATcT),[14,15] the enthalpies of formation for many gas-phase species are now known with sub kJ/mol accuracy at 2σ uncertainty, which is more than adequate for most microkinetic applications. When the enthalpies of formation for the reference reactants are obtained from the ATcT, the uncertainty in $\Delta_{\mathrm{f}}H^{\mathrm{P}}$ is dominated by the error in the computed reaction enthalpy, $\Delta H_{\mathrm{rxn}}^{\mathrm{QM}}$. For molecular systems, various high-level QM methods are capable of computing the reaction enthalpies and, thence, enthalpies of formation with an astonishing accuracy of $< \pm 1\,\mathrm{kJ\,mol^{-1}}$.[16–20]

For chemical species adsorbed on metal surfaces, however, the situation is considerably more complicated. At present, the coupled cluster methods comprising the heart of the aforementioned high-level QM methods are, at best, impractical.[13] Instead, the current state of the art in computational heterogeneous catalysis on transition metals remains density functional theory (DFT) with a generalized gradient approximation (GGA).[21–24] These methods are typically assumed to provide heats of adsorption, ΔH_{ads}, with uncertainties of $\pm 30\,\mathrm{kJ\,mol^{-1}}$.[9] This uncertainty makes it challenging to reach definitive conclusions about reaction pathways in complex networks and the general activity of a specific catalyst facet.[4,25–27]

However, even if one were to accept the current restriction to GGA-DFT for adsorbate thermophysical properties, that does not necessarily imply that the resulting enthalpies of formation will be limited to accuracy on the order of $\pm 30\,\mathrm{kJ\,mol^{-1}}$. One can look at the history of methods for molecular systems for guidance, where similar uncertainty limits were once commonplace. To overcome these uncertainties, Pople and co-workers[28,29] developed an *isodesmic* approach to compute enthalpies of formation, which conserves the bond types between reactants and products in the reference reaction. More elaborate schema were developed to conserve hybridization, which are classified as *homodesmotic* reactions.[30] The overarching goal of all these methods is to devise reactions that increase error cancellation. A corollary of increasing the size of the preserved molecular fragments or functional groups is that the corresponding reaction enthalpy in Equation (2) approaches zero. Deriving these reactions requires extensive chemical knowledge, as there are many possible sets of reference species.[28,30,31] Raghavachari and co-workers developed an elegant method to determine the hierarchy of reference reactions classified by Wheeler et al.,[30,32] called the connectivity-based hierarchy (CBH).[31,33] The CBH method provides a systematic and automated approach for increasing the size of the molecular fragments that are conserved in the reference reaction. It alternates between atom-centric and bond-centric conservation schema, with each new expansion represented by a rung, CBH-n, with $n = 0$, 1, 2, 3, and higher. Climbing the CBH rungs leads to increasing error cancellation for a given QM method and minimizes the uncertainty in the computed enthalpy of formation, as shown for gas-phase systems.[33–37]

In the present work, we apply, for the first time, a structure-based error cancellation technique for adsorbates in heterogeneous catalysis. We adapt the CBH method to automatically derive a hierarchy of reference reactions for a test set of adsorbates on Pt(111). By combining experimental heats of adsorption for all possible bond types with gas-phase enthalpies of formation from the ATcT, we create a basis of accurate reference enthalpies of formation for adsorbates. These experimental enthalpies of formation, in conjunction with the isodesmic reactions, enable us to compute more accurate enthalpies of formation of adsorbates from GGA-DFT energies. The resulting thermochemical network represents a breakthrough in

combining experimental adsorption data with electronic structure calculations for computing enthalpies of formation for adsorbed species on transition metals.

Methods

Connectivity-Based Hierarchy

The connectivity-based hierarchy provides the reactions for the various degrees of bonding and hybridization conservation in an automated framework and was used extensively for large organic molecules.[31,33,36] The degrees of conservation can be classified as: conservation of spin pairs (*isogyric*, CBH-0), bond types (*isodesmic*, CBH-1), immediate connectivity of the heavy atoms (*hypohomodesmotic* or *isoatomic*, CBH-2), and immediate connectivity of the bonds (*hyperhomodesmotic*, CBH-3).[31,33] Although higher levels of this scheme are theoretically possible, the adsorbates in the present work are too small to climb to higher rungs. The CBH methodology is well established for gas-phase molecules, but it has yet to be extended to the complex configurational space of adsorbates, *i.e.* considering the binding to the catalyst surface.

Adsorbates can have a variety of configurations on the catalyst surface, as illustrated in Figure 1: multiple covalent bonds with a surface atom (Figure 1a), branching points (Figure 1b), multiple binding sites (Figure 1c) or adsorb via physisorption through dispersion interactions (Figure 1d). We focus solely on the Pt(111) facet in this work; however, the developed CBH methodology works for any surface, including metal oxides and zeolites, as long as a Lewis or Kekulé structure-based representation of the adsorbate with its bonds can be created. The CBH scheme is explained in detail for adsorbed 1-propyl ($^*CH_2CH_2CH_3$), which is a linear monodentate adsorbate on Pt(111) (see Figure 1a). The method works for all possible adsorbate configurations illustrated in Figure 1, including adsorbates with heteroatoms and is discussed in the SI in detail. An in-house Python code was developed to construct the reactions for the CBH rungs automatically.

Monodentate adsorbate The hierarchy of the reference reactions is summarized in Figure 2. In the isogyric reaction at CBH-0, each heavy atom from the adsorbate is extracted and completely hydrogenated, *e.g.* a C atom is saturated to CH_4. All fragments of the adsorbate are near the catalyst surface, which induces dispersion interactions. Instead of using the energy of CH_4 in the gas-phase, as would be the case following the standard CBH approach,[33] it is assumed that CH_4 is physisorbed on the surface, and we use CH_4^* accordingly. A higher amount of error cancellation can be expected when assuming physisorbed species, since the typical DFT functionals that perform well for adsorbates are often less accurate at predicting gas-phase energies.[9,38–40] Following the formalism, the adsorption site is treated as a single Pt atom that can have either single, double, or triple bonds that can be saturated with H, too. The reaction is then balanced with the required amount of H_2^*.

The first CBH rung above CBH-0 is an isodesmic scheme, where the molecule is separated according to the bonds, resulting in 2 C-C single bonds ($CH_3CH_3^*$) and 1 Pt-C single bond ($^*CH_3$). Decomposing the adsorbate into larger fragments leads to overcounting of some of

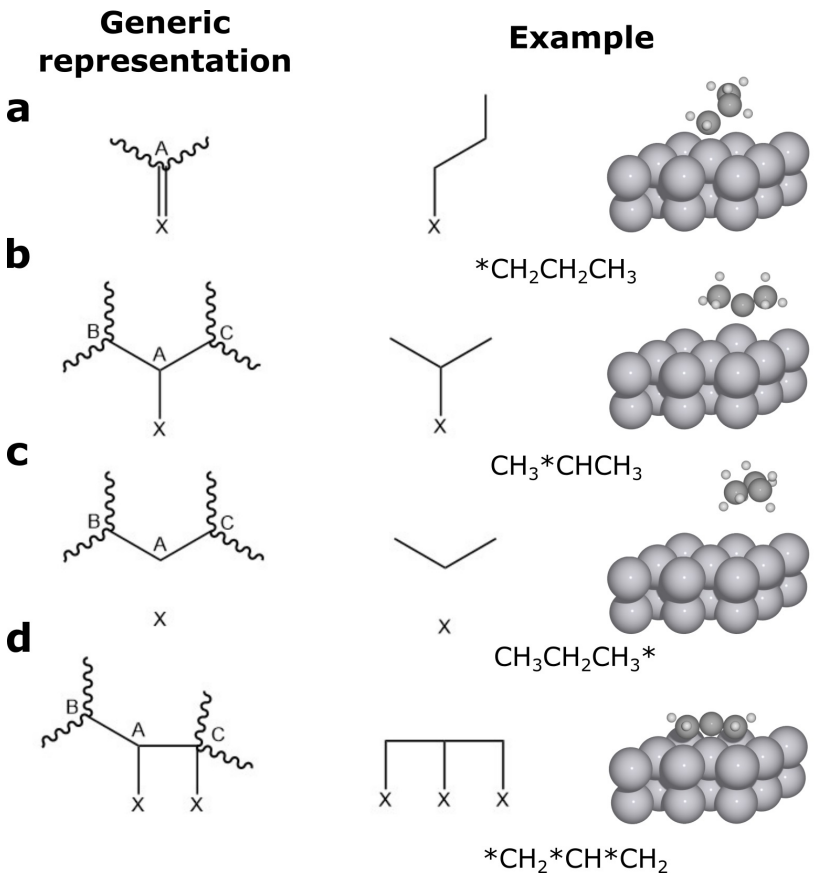

Figure 1: Generic representation of various possible adsorbate configurations on an adsorption site X and images of example structures. a) Adsorbates can bind to the surface with single, double or triple covalent bonds (*e.g.* $^{*}CH_2CH_2CH_3$). b) Adsorbates can have multiple branching points (*e.g.* $CH_3^{*}CHCH_3$). c) Physisorbed species interact through dispersion effects with the surface (*e.g.* $CH_3CH_2CH_3^{*}$). d) Multidentate adsorbates have multiple binding sites with the surface (*e.g.* $^{*}CH_2^{*}CH^{*}CH_2$). The possible extension of the generic molecule is indicated by wiggly lines and A, B, C are generic representations for heavy (non-hydrogen) atoms.

the atoms, as can be seen in the overlap of the fragments in Figure 2, which requires balancing with the appropriate number of CH_4^{*} in this case. As detailed in ref. 33, it is possible to balance these reactions automatically in a systematic approach by moving the products from the previous rung to the reactant side. Terminal moieties of the adsorbate are treated as atom-centric at this level, since they do not have a second bond to another heavy atom. The reader is referred to the SI for the reaction equations with intermediate steps and a more detailed description. At the CBH-2 level, each atom is considered with its immediate bonds to adjacent atoms, resulting in a hypohomodesmotic reaction. $^{*}CH_2CH_2CH_3$ consists of a Pt−C−C fragment (adsorbed ethyl $^{*}CH_2CH_3$) and a C−C−C chain (physisorbed propane $CH_3CH_2CH_2^{*}$). The hypohomodesmotic reaction is balanced with $CH_3CH_3^{*}$ from the CBH-1 rung. It is not possible to ascend the CBH ladder beyond CBH-2 to preserve more of the target adsorbate's structure without reaching the target itself.

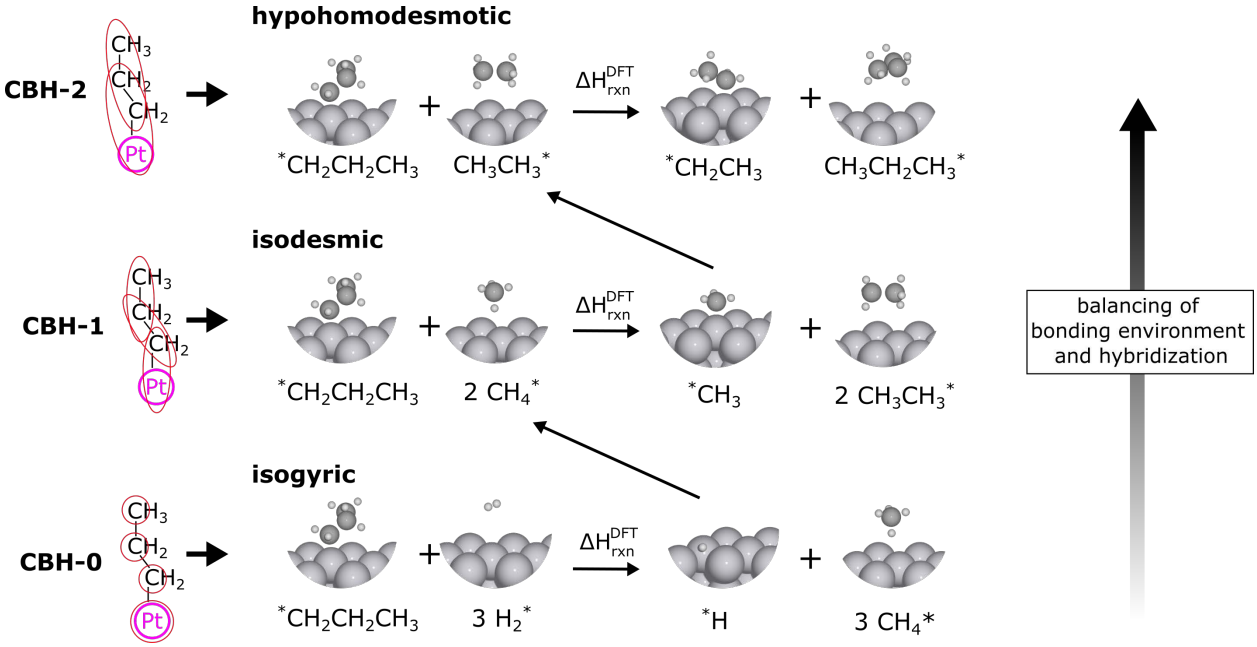

Figure 2: a) Schematic illustration of the generalized connectivity-based hierarchy for adsorbates demonstrated for 1-propyl adsorbed on Pt(111) ($^*CH_2CH_2CH_3$). Not all intermediate reactions are displayed in the manuscript for clarity and the reader is referred to the SI for the details on the derivation of the CBH reactions.

At the isodesmic level (CBH-1), all $C_xH_yO_z$ adsorbates can be decomposed into 10 fragments representing all the possible bond types, shown in Figure 3. These fragments are identical for other (transition) metal surfaces due to the generic nature of the method, but the addition of other heteroatoms would lead to different fragments. The hypohomodesmotic scheme at the CBH-2 level requires considerably more species to account for the increasing complexity in the configuration of the bonding environment and hybridization (see Figure S1).

Electronic Structure Method

We investigated a set of 60 adsorbates on Pt(111) used in the database of the Reaction Mechanism Generator (RMG)[41–43] to test the CBH method, containing all $C_xH_yO_z$ adsorbates with no more than 2 heavy (non-hydrogen) atoms[40] and an additional 40 adsorbates with up to 4 heavy atoms.[3] The electronic structure calculations were conducted with QuantumEspresso (QE)[44,45] using the BEEF-vdW functional.[46] All structures from Blondal et al.[40] were re-relaxed on the optimized slab from the QE DFT calculations to obtain a set of consistent DFT energies. A (3×3×4) Pt(111) unit cell with an optimized lattice constant was used, which corresponds to a coverage of $1/9^{\text{th}}$ of a monolayer. Mazari-Vanderbilt smearing is applied with a value of 0.02 Ry. Adsorbates were relaxed, together with the 2 top layers of the slab, to within 0.025 eV $Å^{-1}$, with an energy cutoff of 50 Ry on a (5×5×1) Monkhorst-Pack mesh. The single-point energies were calculated at identical settings, with an increased energy cutoff of 60 Ry. Vibrational analysis was conducted through ASE, and imaginary frequencies were set to 12 cm^{-1}, similar to ref. 47. More details on the DFT calculations are

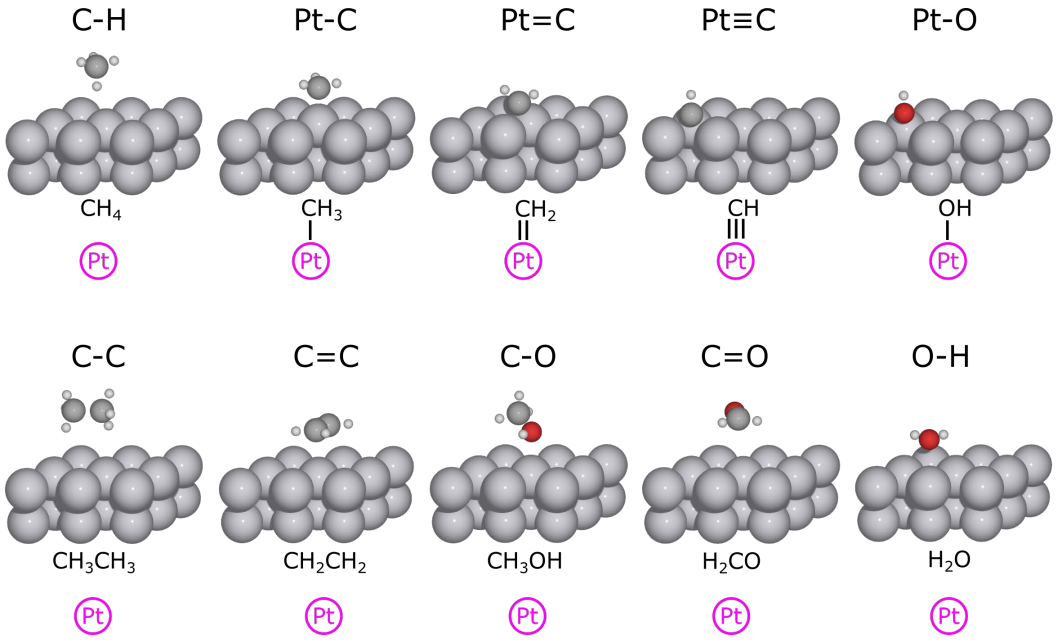

Figure 3: Adsorbate fragments required for the construction of the isodesmic bond separation reactions (CBH-1) for the investigated adsorbates on Pt(111) within this work.

reported in ref. 3, and the obtained raw DFT energies are provided in Table S1.

Experimental Enthalpies of Formation

The CBH scheme requires accurate enthalpies of formation for the reference species that are used in the hypothetical reactions. Currently, neither experimental nor independent QM enthalpies of formation that are required for the construction of the CBH-2 or CBH-3 rung are available. Formation enthalpies of all fragments required for the construction of the isodesmic reactions at the CBH-1 level were derived from experimental heats of adsorption.[9,48–52] The experimental heats of adsorption are assumed to be accurate to within $\pm 10\,\mathrm{kJ\,mol^{-1}}$.[8,50] The species, along with the reactions and measured heat of adsorption ΔH_{ads}, are summarized in Table 1. Enthalpies of formation are obtained from the heats of adsorption by combining them with the tabulated gas-phase enthalpies of formation from the ATcT.[14,15] The method to compute $\Delta_{\mathrm{f}}H^{\mathrm{exp}}_{0\mathrm{K}}$ along with the necessary temperature corrections are discussed in detail in the SI and all scripts are available in ref. 53. The results are reported in Table 1.

Results

The isogyric (CBH-0), isodesmic (CBH-1), hypohomodesmotic (CBH-2) and hyperhomodesmotic (CBH-3) reactions for all 60 adsorbates are summarized in Table S6-S8. The highest possible rung depends on the size and configuration of the target adsorbate. Figure 4a shows the computed reaction enthalpies for the various CBH rungs of the adsorbates that were used as examples in Figure 1. The largest absolute value of the reaction enthalpy is observed for the isogyric reaction, which has the least amount of preservation of the bonding

Table 1: Measured heats of adsorption on Pt(111) and derived enthalpies of formation at 0 K for the species that were used as fragments for the bond types to construct the isodesmic bond separation reactions (CBH-1 rung). All enthalpies are in kJ mol^{-1}.

species	bond type	reaction	ΔH_{ads}	T / K	$\Delta_{\mathrm{f}}H^{\mathrm{exp}}_{0\mathrm{K}}$	ref.
$^{*}CH_3$	Pt–C	$CH_3I + 2\,^{*} \rightleftharpoons {}^{*}CH_3 + {}^{*}I$	-210[c]	320	-47.2	51
$^{*}CH$	Pt≡C	$CH_2I_2 + 4\,^{*} \rightleftharpoons {}^{*}CH + {}^{*}H + 2\,{}^{*}I$	-470[c]	210	-35.8	54
$^{*}CH_2$[a]	Pt=C	$CH_2I_2 + 3\,^{*} \rightleftharpoons {}^{*}CH_2 + 2\,{}^{*}I$	-	-	46.5	54
CH_3OH^{*}	C–O	$CH_3OH + {}^{*} \rightleftharpoons CH_3OH^{*}$	-263	100	-245.0	52
$CH_2CH_2^{*}$	C=C	$CH_2CH_2 + {}^{*} \rightleftharpoons CH_2CH_2^{*}$	-40	112	22.1	55
H_2CO^{*}	C=O	$H_2CO + {}^{*} \rightleftharpoons H_2CO^{*}$	-55.2	235	-159.3	48
$CH_3CH_3^{*}$	C–C	$CH_3CH_3 + {}^{*} \rightleftharpoons CH_3CH_3^{*}$	-28.5	106	-96.0	9
CH_4^{*}	C–H	$CH_4 + {}^{*} \rightleftharpoons CH_4^{*}$	-15	63	-81.3	9
H_2O^{*}	O–H	$H_2O + {}^{*} \rightleftharpoons H_2O^{*}$	-31.3	120	-267.9	9
$^{*}OH$[b]	Pt–O	$H_2O^{*} + {}^{*} \rightleftharpoons {}^{*}OH + {}^{*}H$	68	298	-164.7	50
$^{*}H$	Pt–H	$H_2 + 2\,^{*} \rightleftharpoons 2\,{}^{*}H$	-72	300	-32.7	9

[a] The enthalpy of formation of $^{*}CH_2$ originally measured by Wolcott et al.[54] was 181 kJ mol^{-1}, but this enthalpy of formation is subjected to adsorbate-adsorbate interactions from co-adsorbed *I. Instead they estimate the enthalpy of formation based on a measured activation barrier for the dissociation of $CH_3^{*} + 2\,^{*} \rightleftharpoons {}^{*}CH + 2\,{}^{*}H$ with 61 kJ mol^{-1}.[56] This estimate provides the upper limit for the enthalpy of formation of $^{*}CH_2$ as described in ref 54.

[b] The enthalpy of formation of *OH was calculated from an experimental reaction enthalpy taken from Karp et al.[50]

[c] The measured heat of adsorption of these reactions was corrected by 2 kJ mol^{-1} compared to the original paper due to a systematic error as described in ref. 8.

environment. With each successive CBH rung, the absolute value of the reaction enthalpy decreases, which leads to more accurate enthalpies of formation. This behavior is observed for organic species in the gas phase as well.[33,40] The trend from the example adsorbates is confirmed by the average reaction enthalpies for the CBH levels in Figure 4b, demonstrating an increasing cancellation of errors at higher CBH rungs. A systematic error cancellation is also observed for the zero-point vibrational energies (ZPE), since larger fragments exhibit similar vibrational modes as the target, which leads to an almost complete cancellation at the CBH-3 level.[32]

A structural complexity that differs from the gas-phase CBH method is the binding to the catalyst surface. For adsorbates with double or triple bonds to the surface or other heavy atoms, the CBH-0 (isogyric) approach can lead to inconsistencies with respect to the number of Pt atoms in the GGA-DFT calculations (see SI for an in-depth explanation). This inconsistency can be resolved in an *ad hoc* manner by including the DFT energy for a certain number of vacant slabs. However, more importantly, this inconsistency is resolved completely when one moves to the CBH-1 (isodesmic) level, and no *ad hoc* corrections are

required.

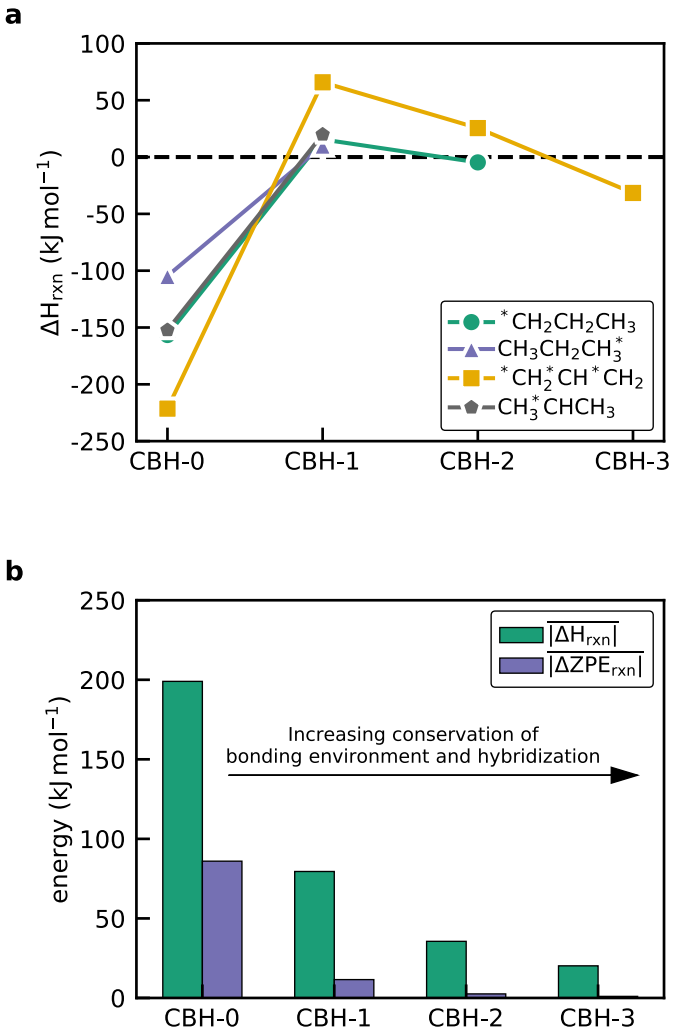

Figure 4: a) Reaction enthalpy for the different CBH rungs for the example adsorbates. See Methods section and SI for the corresponding reaction equations. b) Average absolute reaction enthalpy ΔH_{rxn} and average change in the zero-point energy $\Delta\text{ZPE}_{\text{rxn}}$ of the reference reactions for all adsorbates that could be computed with the various CBH rungs.

Ideally, the highest possible CBH rung would be used to compute the enthalpy of formation of an adsorbate, since it exploits the highest possible cancellation of error. However, it is only possible to climb to the highest CBH rungs for which accurate and *independent* reference enthalpies of formation are available. In this study, we only use the experimental values for the CBH-1 level, and we do not add additional values for the higher rungs, due to the limited amount of available data. Using these fragments in the hypohomodesmotic reactions or beyond will result in a linear combination of the lower CBH rungs; these higher rungs may decrease in reaction enthalpy (see Table S2), but they do not lead to changes in the enthalpy of formation. The proposed methodology joins the available experimental data for reference species with the DFT calculations to compute the enthalpies of formation of adsorbates that

are difficult to assess experimentally. Thereby, we effectively combine DFT with experiments in a unified thermochemical network.

An enthalpy diagram for the computation of the enthalpy of formation within this CBH approach is illustrated in Figure 5 for $^{*}CH_2CH_2CH_3$. The isodesmic reaction to determine the enthalpy of formation of $^{*}CH_2CH_2CH_3$ is $^{*}CH_3 + CH_3CH_3^{*} - 2\,CH_4^{*} \longrightarrow {}^{*}CH_2CH_2CH_3$. Consequently, the enthalpy of formation of 1-propyl is anchored to $^{*}CH_3$, $CH_3CH_3^{*}$, and CH_4^{*} via the reaction enthalpy from the DFT energies. The reference species are linked to the enthalpy of formation of the experimental gas-phase precursor from the ATcT, which are CH_3I, CH_3CH_3, and CH_4, respectively (see Table 1).

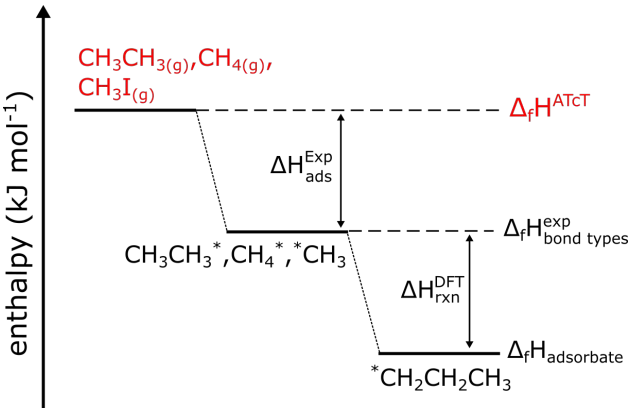

Figure 5: Enthalpy diagram to derive the enthalpy of formation of an adsorbate (in this case, $^{*}CH_2CH_2CH_3$) from an isodesmic reaction via the connectivity-based hierarchy in combination with experimental heats of adsorption of the bond types.

Comparison with Prior Methods

Unfortunately, the availability of suitable data to benchmark the proposed methodology is quite limited; instead, we choose to compare the derived enthalpies of formation with another method, which was previously developed by the authors.[40] In our previous approach, the enthalpy of formation of the adsorbate is computed from an adsorption reaction of a gas-phase precursor, where the heat of adsorption is derived from DFT. Combining the heat of adsorption with the enthalpy of formation of the precursor from an existing gas-phase thermochemical database ensures a thermodynamically consistent enthalpy of formation of the adsorbate. Not all enthalpies of formation of the precursors are available, as many adsorbates form only meta-stable structures in the gas phase. Instead, the enthalpy of formation is determined from an isogyric gas-phase reaction, similar to the CBH-0 rung. This approach leads to a cancellation of the DFT energy of the gas-phase precursor, since it appears in the heat of adsorption and the reaction enthalpy.[40] Consequently, the method produces a fully consistent TN, where every adsorbate is anchored to the ATcT via CH_4, H_2O, and H_2. We denote this method as the "adsorption reaction" approach. It was used to construct thermodynamically consistent microkinetic models that could successfully describe experimental results.[3,4,25,26,40,57–59] Nonetheless, the computed enthalpy of formation is subjected to the large uncertainties inherent to the DFT energies, as there is no cancellation of errors in the

heat of adsorption. It further depends on the accuracy of the DFT energies for the fragments of the isogyric reaction in the gas-phase, which can contain considerable errors.[39,60]

Benchmark

With experimental enthalpies of formation for the bond types, the enthalpy of formation of the target adsorbate can now be computed through the isodesmic bond separation reactions derived at the CBH-1 level. The derived enthalpies of formation from the isodesmic bond separation reactions are compared with available experiments as a benchmark in Table 2. Karp et al.[52] measured an enthalpy of formation of methoxy ($^{*}OCH_3$) of $-161.2\,\mathrm{kJ\,mol^{-1}}$ on Pt(111), which compares to $-147.5\,\mathrm{kJ\,mol^{-1}}$ with the adsorption reaction approach and $-163.6\,\mathrm{kJ\,mol^{-1}}$ with the isodesmic reaction. The difference in the enthalpy of formation for formic acid is increased to $8.5\,\mathrm{kJ\,mol^{-1}}$ from $0.1\,\mathrm{kJ\,mol^{-1}}$, but it is still within the experimental uncertainty. Excellent agreement is obtained for $CH_3CH_2CH_3^{*}$, which is within $\pm 2\,\mathrm{kJ\,mol^{-1}}$ for both approaches. This result also highlights that the previously developed method produces accurate enthalpies of formation of the adsorbate with a closed-shell precursor.

The enthalpy of formation of monodentate formate ($-347.3\,\mathrm{kJ\,mol^{-1}}$) is significantly overestimated by both approaches, with $-380\,\mathrm{kJ\,mol^{-1}}$ (CBH-1) and $-366.2\,\mathrm{kJ\,mol^{-1}}$ (adsorption reaction). However, the experimental enthalpy of formation of monodentate formate was obtained at a coverage of 1/4 ML, so lateral interactions could destabilize the adsorbed formate significantly;[61] consequently, the actual enthalpy of formation of formate at a lower coverage could be closer to the predicted theoretical values. The reaction enthalpy of the isodesmic reaction for formate is $-160\,\mathrm{kJ\,mol^{-1}}$, which is considerably higher than the average over all isodesmic reactions (see Figure 4). A large reaction enthalpy indicates comparatively little error cancellation and thus a higher uncertainty in the enthalpy of formation. Moreover, the isodesmic reaction of $HC(O)^{*}O$ has more fragments than any other isodesmic reaction, which could compound additional uncertainties.[32] It would be preferred to climb to the hypohomodesmotic reaction, as it leads to a significant decrease in the reaction energy ($-25\,\mathrm{kJ\,mol^{-1}}$).

The reaction enthalpy can be used as a measure for the effectiveness of the error cancellation, where reaction enthalpies close to zero indicate the highest amount of cancellation. Overall, the small benchmark study shows that the CBH approach provides enthalpies of formation that are well within the experimental uncertainty of $\pm 10\,\mathrm{kJ\,mol^{-1}}$ for the adsorbates, except for $HC(O)^{*}O$ due to the discussed reasons. The lack of experimental or highly accurate theoretical data of larger adsorbates prevents further benchmark tests of the CBH approach at the time of this publication.

Due to the limited availability of benchmark values, either experimentally measured or obtained from more accurate QM methods, we compare the enthalpy of formation from the CBH approach with the values from the adsorption reaction approach of Ref. 40 (see Figure 6). Computed enthalpies of formation from the isodesmic reactions should theoretically produce enthalpies of formation closer to the actual enthalpy of formation. It is derived from more accurate surface reaction energies instead of heats of adsorption, which contain

Table 2: Comparison of experimental enthalpies of formation with the calculated enthalpies from the adsorption reaction and the CBH approach. All values are in kJ mol^{-1} and at a temperature of 0 K. The details on the experimental results is provided in the SI.

species	isodesmic reaction	ΔH_{rxn}	$\Delta_{\mathrm{f}}H^{\mathrm{exp}\,\dagger}$	$\Delta\Delta_{\mathrm{f}}H^{\mathrm{CBH\text{-}1}}$	$\Delta\Delta_{\mathrm{f}}H^{\mathrm{direct}}$
$^{*}OCH_3$	$^{*}OCH_3 + H_2O^{*} \longrightarrow {}^{*}OH + CH_3OH^{*}$	21.8	-161.2[52]	-2.4	13.7
$HC(O)OH^{*}$	$HC(O)OH^{*} + CH_4^{*} \longrightarrow CH_3OH^{*} + H_2CO^{*}$	113.9	-428.4[52]	-8.5	0.1
$CH_3CH_2CH_3^{*}$	$CH_3CH_2CH_3^{*} + CH_4^{*} \longrightarrow 2\,CH_3CH_3^{*}$	10.1	-122.7[9]	1.9	1.4
$HC(O)^{*}O$	$HC(O)^{*}O + H_2O^{*} + CH_4^{*} \longrightarrow {}^{*}OH + CH_3OH^{*} + H_2CO^{*}$	160.2	-347.3[61]	-32.7	-18.9

† The experimental enthalpies of formation are derived from the measured heats of adsorption reported in the cited references and corrected to a temperature of 0 K as described in the SI.

the uncertainties of the gas-phase DFT energies.[39,60] The change in the enthalpy of formation of most adsorbates is within ± 30 kJ mol^{-1}, which is the accuracy of the GGA functionals, but there are some adsorbates for which a larger deviation is observed. The mean absolute deviation (MAD) across all 60 adsorbates between both methods amounts to 21 kJ mol^{-1}. The enthalpy of formation from the CBH is mostly decreased to more negative values compared with the adsorption reaction approach. Experimental enthalpies of formation of the fragments for the bond types are always more negative (stabilized) than the values from the adsorption reaction approach (see Table S5), except for $^{*}CH_2$, which explains the observed shift in the enthalpy of formation. This deviation of experimental values and from the adsorption reaction approach can point to a constant offset for the DFT energy of the fragments for the isogyric reaction in the gas phase, which often necessitates the usage of correction factors to better match the experiments with theory[39] or in the BEEF-vdW functional in general.

Figure 6 presents the change in the enthalpy of formation, separated by the type of surface bond. Large changes are apparent for all cases. Bidentate adsorbates contribute the most to the deviation, with a MAD of 33 kJ mol^{-1}, while the difference is the smallest for the physisorbed species (10 kJ mol^{-1}) (see Figure S2). The BEEF-vdW functional is trained to account for dispersion effects, so it can be expected that physisorbed adsorbates are accurately described.[46] This attribute of the BEEF-vdW also supports the observation that the adsorption reaction approach works particularly well for adsorbates with a closed-shell precursor. The enthalpy of formation of this precursor is determined through an isogyric reaction from the ATcT database, which performs better for closed-shell species than for the open-shell radicals.[40]

Adsorbates that bind to Pt through C with a double bond, such as $^{*}CH_2$, exhibit the highest deviation from the adsorption reaction approach, with a MAD of 49 kJ mol^{-1}. This deviation is partially related to the difference between the experimental and the adsorption reaction value for the Pt=C bond ($\Delta\Delta_{\mathrm{f}}H = 40$ kJ mol^{-1}, see Table S9). Unfortunately, the experimental enthalpy of formation of $^{*}CH_2$ has a higher uncertainty than the other experimental values; it is challenging to measure experimentally, and the current value is based upon an upper limit estimate[54] (see Table 1). The biggest difference for a single adsorbate occurs for the two bidentate species $^{*}C^{*}C$ and $^{*}CH^{*}CH$, with approx. 100 kJ mol^{-1}. These adsorbates have two fragments of methylidene contributing to this difference, since they have two Pt=C

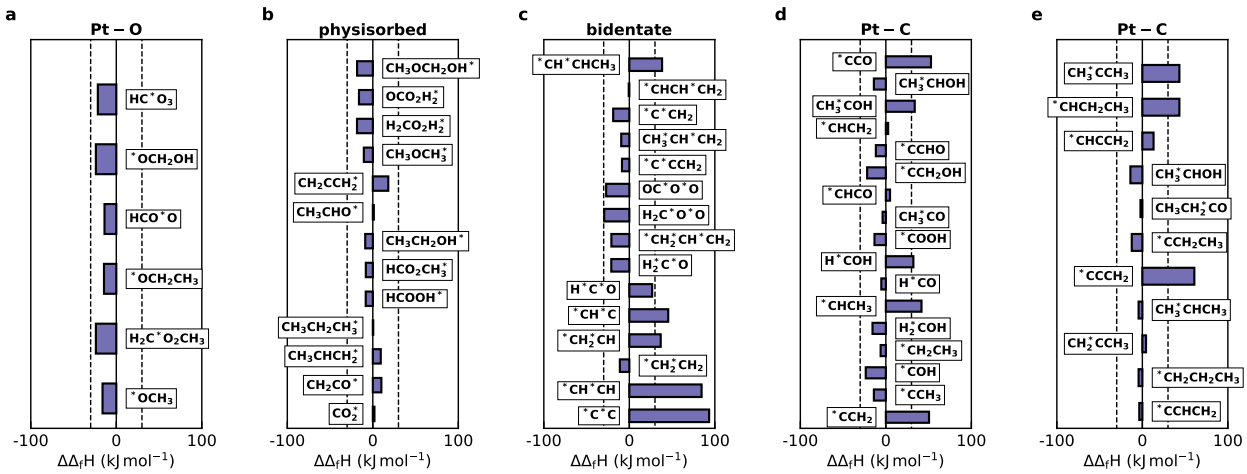

Figure 6: Comparison of the change in the enthalpy of formation at 0K of the adsorbates from the CBH-1 method compared to the adsorption reaction approach of Blöndal et al.[40] a) Adsorbates that bind through oxygen, b) physisorbed species, c) bidentate adsorbates binding either through carbon or oxygen, d) adsorbates with no more than 2 C atoms binding through carbon, and e) adsorbates with 3 C atoms binding through carbon. The dashed line highlights a range of $\pm 30\,\mathrm{kJ\,mol^{-1}}$ which is assumed to be the uncertainty of the GGA functionals. Although the enthalpies of formation of the adsorption reaction approach are used as a reference, it does not imply that these are more accurate enthalpies of formation.

bonds. Another obstacle for these two bidentate adsorbates, as well as the related bidentate $^{*}C^{*}CH$, is that there are resonance structures, *i.e.* different Kekulé structures that fulfill the octet rule without a clear geometrical distinction. Different Kekulé structures leads to different isodesmic reactions and, consequently, different enthalpies of formation (see the SI for a more in-depth discussion). However, the topic of resonance structures goes beyond the scope of the paper and is the subject of a companion work by the authors.

Test Case: Propane Dehydrogenation

A case study for a propane dehydrogenation mechanism is illustrated in Figure 7 to demonstrate the difference between both approaches to derive the enthalpies of formation. The mechanism assumes that propane is dehydrogenated on Pt(111) according to the following elementary steps:

$$
\begin{aligned}
CH_3CH_2CH_3(g) + {}^{*} &\rightleftharpoons CH_3CH_2CH_3^{*} \\
CH_3CH_2CH_3^{*} + {}^{*} &\rightleftharpoons {}^{*}CH_2CH_2CH_3 + {}^{*}H \\
{}^{*}CH_2CH_2CH_3 + 2\,{}^{*} &\rightleftharpoons {}^{*}CH_2^{*}CHCH_3 + {}^{*}H \\
{}^{*}CH_2^{*}CHCH_3 &\rightleftharpoons CH_2CHCH_3(g) + 2\,{}^{*} \\
2\,{}^{*}H &\rightleftharpoons H_2(g) + 2\,{}^{*}
\end{aligned}
$$

which is the main pathway for propene formation discussed by Saerens et al.[62] In our comparison, we do not assert that this mechanism the only important pathway, nor do we attempt to provide new insights in this important process. In Figure 7a, the enthalpy of formation is derived via the adsorption reaction approach through the heat of adsorption of a gas-phase precursor. The enthalpy of formation of the gas-phase precursor should be identical to the enthalpy of formation reported in the ATcT database, if a value is available. An isogyric reaction for the gas-phase precursor creates imbalances in the bonding environment,[33] which is why there can be inconsistencies in the enthalpies. The enthalpy of formation at 0 K of propane from the ATcT is $-82.7\,\mathrm{kJ\,mol^{-1}}$, whereas the value predicted by the isogyric reaction is $-98\,\mathrm{kJ\,mol^{-1}}$. Surprisingly, the predicted enthalpy of formation for $CH_3CH_2CH_3^*$ from the adsorption reaction approach is close to the experimental value (see Table 2). In contrast, the enthalpy of formation of the intermediates is computed through the isodesmic reaction in Figure 7b, and no gas-phase species are involved. Thus, this approach reduces the required computational costs for the electronic structure calculations by eliminating the need to compute the gas-phase precursor completely, which is often the biggest source of error.[39,40]

The dissociation of $CH_3CH_2CH_3^*$ is predicted to be endothermic, which is related to the enthalpy of formation of $^*CH_2CH_2CH_3$ ($\Delta_f H_{0K} = -88\,\mathrm{kJ\,mol^{-1}}$) as well as $^*H$ ($\Delta_f H_{0K} = -23.4\,\mathrm{kJ\,mol^{-1}}$). $CH_3CH_2CH_3^*$ is energetically favored according to the computed enthalpies of formations, whereas we expect it to be exothermic since dissociative adsorption is reported in experiments.[63] Using the CBH method for $^*CH_2CH_2CH_3$ ($\Delta_f H_{0K} = -93\,\mathrm{kJ\,mol^{-1}}$) in conjunction with the experimental value for $^*H$ ($-32.7\,\mathrm{kJ\,mol^{-1}}$) is enough to change the sign of the reaction enthalpy, which makes the dissociation energetically favorable. Consequently, $^*CH_2CH_2CH_3$ is more stable than $CH_3CH_2CH_3^*$. This change in the relative stability of adsorbed propyl has significant effects on the predictions of the microkinetic model about the dehydrogenation activity of the Pt(111) facet. Reaction energies of the isodesmic reactions for $CH_3CH_2CH_3^*$ and $^*CH_2CH_2CH_3$ are fairly low and point to a high error cancellation and presumably accurate enthalpies of formation.

Discussion

One of the well-known problems of the common GGA functionals is the overprediction of the binding energy of adsorbates with an OCO backbone, such as CO_2^*.[39] An enthalpy of formation was computed with the adsorption reaction approach of $-468\,\mathrm{kJ\,mol^{-1}}$. With the isodesmic reaction, $2\,H_2CO^* - CH_4^* \longrightarrow CO_2^*$, a similar enthalpy of formation is predicted for CO_2^*, $-466\,\mathrm{kJ\,mol^{-1}}$, which implies that CO_2^* still binds strongly to the Pt(111) surface, in direct contrast to experimental results.[64] The reaction enthalpy for the isodesmic reaction is $-229\,\mathrm{kJ\,mol^{-1}}$, indicating little-to-no cancellation of error. Since both molecules interact only weakly through dispersion with the Pt(111) surface, their hybridization remains similar to the gas-phase molecule. In the gas phase, the C atom in CO_2 has an *sp* hybridization, whereas it is sp^2 hybridized in H_2CO. The difference in the hybridization results in an imbalance in the reaction energy, and the enthalpy of formation of CO_2 cannot be more accurately estimated via CBH. It is not possible to create a hypohomodesmotic reaction for CO_2^* due to the small size.

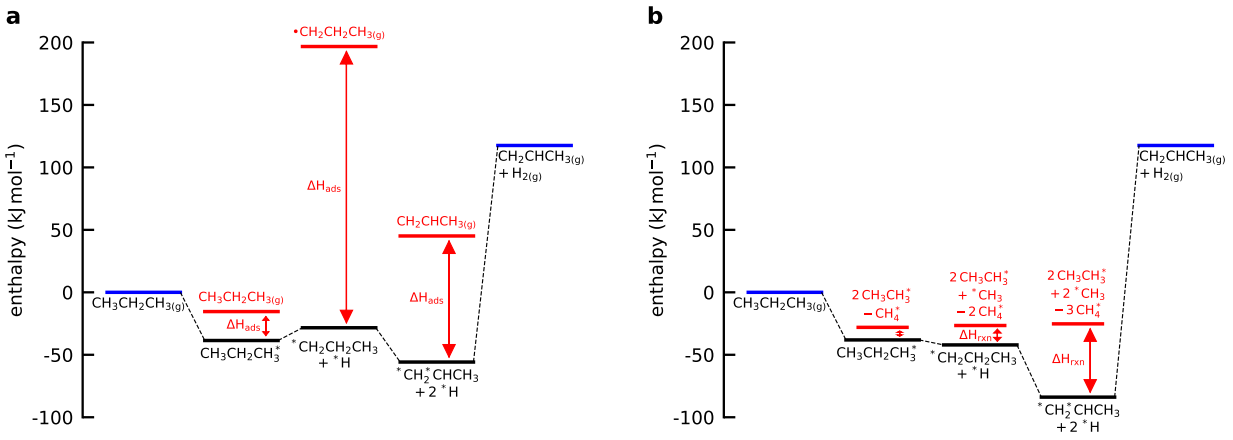

Figure 7: Enthalpy diagram (at 0 K) for the intermediates in a possible pathway in the dehydrogenation of propane over Pt(111) for a) the direct approach through heats of adsorption and b) the connectivity-based hierarchy for adsorbates in combination with experimental enthalpies of formation. The enthalpies of formation of $CH_3CH_2CH_3$(g) and CH_3CHCH_2(g) (blue line) were taken from the ATcT. The red arrows indicate the reference to the existing thermochemical network through a) heats of adsorption and b) enthalpies of surface reactions. No transition states are included in the enthalpy diagram as they are independent of the used method. Note that the enthalpy of formation of the gas-phase precursor in a) for propane and propene is derived through an isogyric reaction of CH_4 and H_2, which differs from the enthalpy of formation from the ATcT. The reference for *H is omitted for clarity.

This particular case highlights one of the shortcomings of the CBH method: for small molecules, it might not be possible to conserve the correct hybridization in all cases, and, thus, the error cancellation is expected to be comparatively low. Even though the error cancellation is low, the method still produces consistent enthalpies of formation comparable with the prior approach. Consequently, whenever the reaction enthalpy is comparatively high at the CBH-1 level, and no higher rungs are possible, the best one can do is to use a more advanced QM method. Conversely, the full power of the CBH approach becomes apparent when the molecules and/or adsorbates are significantly larger than the fragments used to create the isodesmic or hypohomodesmotic reactions, since it allows for more a rigorous conservation of the structure. The CBH approach becomes essential when the molecules get even larger, such as C_5 hydrocarbons and beyond for processes like the Fischer-Tropsch synthesis, where only inexpensive GGA-DFT calculations are feasible.

Thermochemical Networks

Figure 8 presents two different thermochemical networks for the same 60 adsorbates. Figure 8a illustrates the TN obtained by the adsorption reaction to H_2(g), CH_4(g), and H_2O(g) through isogyric reactions;[40] Figure 8b illustrates the TN obtained by the present work, which involves a combination of experimental enthalpies of formation with DFT energies in the error cancellation procedure. In each figure, the vertices represent the enthalpies of formation of either the gas-phase reference species or adsorbates, and the edges represent con-

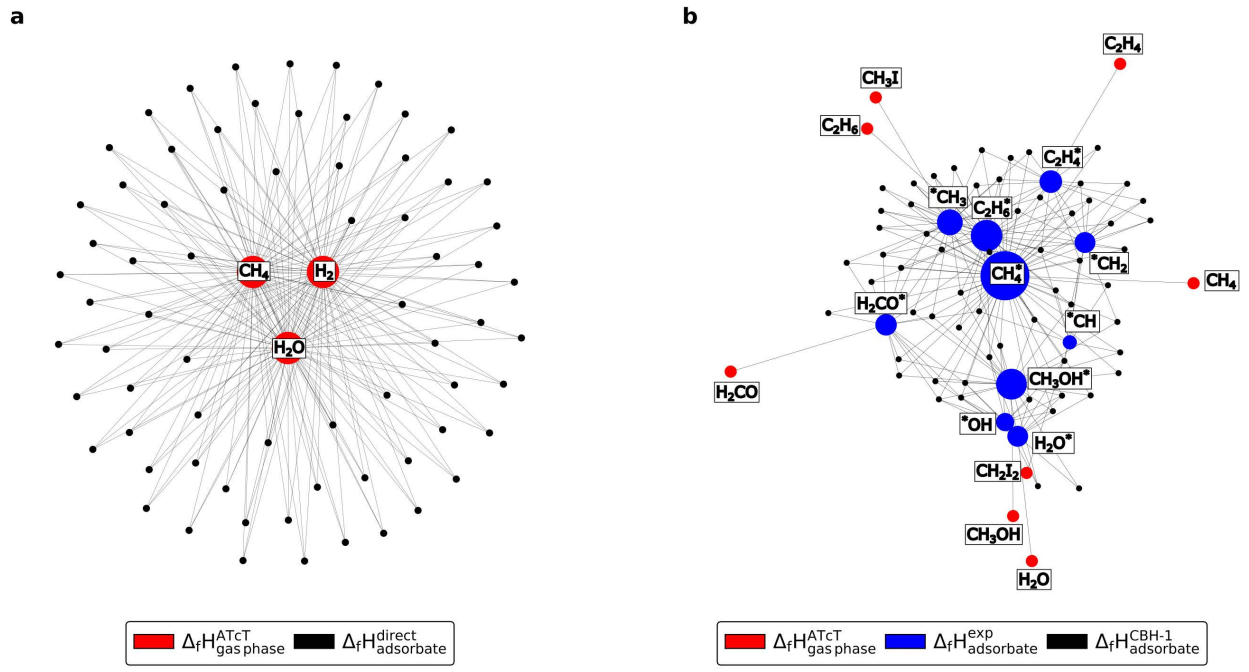

Figure 8: Network representation of the thermochemistry database with the (a) adsorption reaction approach and (b) the proposed procedure of this study with the coupling of experimental and theoretical methods using the connectivity-based hierarchy approach. The size of the nodes indicates how often a species is used as a fragment in the CBH scheme to assess the enthalpy of formation of another adsorbate. Not all node labels are displayed for clarity.

nectivity through either the isogyric gas-phase reaction (Figure 8a) or the isodesmic reaction (Figure 8b); the size of a vertex corresponds to its degree of connectedness within the TN. As is clear from the two figures, the two approaches, though both internally thermodynamically consistent, yield thermochemical networks with remarkably different connectivities.

In Figure 8a, all adsorbates are referenced to H_2, CH_4, and H_2O, which ensures thermodynamic consistency with the gas phase, as demonstrated in previous studies.[3,4,25,57] In this network, there are no connections between adsorbate vertices, and the enthalpies of formation for are completely independent of each other. Consequently, if the enthalpy of formation of an adsorbate is adjusted within the adsorption reaction approach, it can easily be seen that this adjustment does not affect any other species in the TN.

A completely different TN is obtained with the combination of experimental enthalpies of formation and DFT in the CBH scheme, as shown in Figure 8b. All experimental enthalpies of formation of the fragments that are used for the bond types are anchored to gas-phase enthalpies of formation (see Table 1). This approach provides a larger set of anchor points to the ATcT than the isogyric gas-phase reaction, and it uses the measured heats of adsorption. Since the enthalpy of formation of all other adsorbates is derived from the isodesmic bond separation reactions, the experimental enthalpies of formation of the reference adsorbates for the bond types are nodes with many edges to larger adsorbates. The CBH method creates a complex network, with many interconnected nodes that resembles more closely the structure

of the typical TN *e.g.* the ATcT database.[15] Not all of the fragments occur with equal frequencies in the CBH scheme. Adsorbates like CH_4^*, $C_2H_6^*$, and CH_3OH^* are major hubs in this network, while the enthalpy of formation of $^*CH$ is less frequently used, as indicated by the size of the nodes.

One of the major advantages of the new approach is that each node can also be used as an additional anchor point if experimental or more accurate theoretical data become available. In this study, we focused only on deriving enthalpies of formation from the CBH-1 rung. Going beyond the isodesmic reactions towards hypohomodesmotic reactions at the CBH-2 level would add another level of hierarchy to this approach, with additional edges between the adsorbates. However, this expansion of the reference basis requires accurate enthalpies of formation for the diatomic fragments (see Figure S1). Unlike the prior approach, changing the enthalpy of formation or providing an additional anchor point for a higher CBH level will affect all the thermochemistry values through the adjacent edges.

Beyond DFT

The CBH method depends on the chosen anchor points and the accuracy of the experimental data for the bond types, which is usually reported to be within $\pm 10\,\mathrm{kJ\,mol^{-1}}$.[7–9] Most of the experimental heats of adsorption for the small fragments are known with suitably high accuracy, except for the values for physisorbed $CH_2CH_2^*$,[55] H_2CO^*,[48] and $^*CH_2$.[54] The heats of adsorption of these molecules is difficult to measure, since they dissociate upon adsorption or during the temperature programmed desorption, making the measured heats of adsorption a convolution of various elementary steps.[48,49,65,66] Additionally, the π-bonded ethylene is only stable at high coverages, and the corresponding enthalpy of formation might thus be a conservative estimate of the actual value. As these challenges are difficult to overcome experimentally, it will be necessary to determine the enthalpy of formation of these adsorbates either through different experimental references or with highly accurate QM methods, such as quantum Monte Carlo,[67] coupled cluster,[68] and random phase approximation.[69] Changes in the enthalpy of formation of the small fragments due to better QM methods will have a large impact on the entire network. Therefore, all effort should be directed into deriving the enthalpy of formation of these key intermediates that form the central hubs in this TN, either through additional experiments or through advanced QM methods (or both). The approach becomes more powerful when the enthalpies of formation of the fragments at the CBH-2 level are all either available through experiments or higher level of theory methods. A high accuracy is also required for the entropy and heat capacity of the adsorbates to convert between the experimental temperatures and standard conditions, which requires methods that account for anharmonic effects.[6]

The construction of reactions that preserve the structure of a target species via the CBH is strongly interwoven with group additivity methods.[32] Group additivity methods have been employed in heterogeneous catalysis to determine the enthalpies of formation.[11,12] However, the CBH approach is distinctly different, as it still requires and uses electronic structure calculations to increase the accuracy from DFT without raising computational costs. The idea behind group additivity is to circumvent the DFT calculation entirely and to estimate the enthalpy of formation based on the structural decomposition of the target. This decom-

position can also be conducted in a way to conserve bonding environment and hybridization, which will lead to expression similar to the isodesmic or homodesmotic reactions from the CBH. In fact, it would be possible to construct group additivity parameters based on the accurate enthalpies of formation derived via the isodesmic bond separation reactions presented in this work; as done by Ghosh and co-workers[70] for gas-phase molecules.

The CBH approach developed by Raghavachari and co-workers[33] extended in this study to the adsorbate thermochemistry provides an automated way to derive reactions for various degrees of preservation of the bonding environment and hybridization. One of the open tasks is to include additional available experimental data for small adsorbates not explicitly required in the CBH approach, like *H,[65] *CO,[65] and *O[50] through Hess cycles. As the size of reference species increases, there will be the need to ensure the fulfillment of Hess cycles across all possible reaction sequences. This criterion will pose a minimization problem of the linear algebraic equations, which is similar to the ATcT database.[15] The proposed methodology is generic and is expected to work for all metals, crystal facets, oxides, or zeolites, as well as for electrochemical systems. We anticipate that this approach will be of utmost importance to tackle the increasing computational costs for the investigation of larger adsorbates and to reduce the uncertainty associated with GGA-DFT calculations, enabling more sophisticated design of catalytic materials and reactors. Overall, this study provides a significant step forward in constructing a unified thermophysical database for adsorbates.

Conclusion

This work presents the first application of an error cancellation method for the computation of enthalpies of formation for adsorbed intermediates on a heterogeneous catalyst from DFT calculations with increased accuracy. The cancellation of errors from DFT is achieved through an automatic structure-based fragmentation of the target adsorbate using the generalized connectivity-based hierarchy method, which is adjusted and extended for adsorbates on a catalytic surface in this work. The CBH approach combines the fragments in reactions that preserve the bonding environment and hybridization of the target adsorbate. Enthalpies of formation of fragments can be determined from experiments (or more accurate QM methods, when available) and combined with reaction enthalpies from DFT. Therefore, the method will be particularly useful to derive enthalpies of formation of larger adsorbates where high-accuracy QM calculations become prohibitively expensive and comparatively cheap DFT calculations can be used instead. The outlined approach to compute the enthalpy of formation through this method no longer necessitates the computation of the adsorbate precursor in the gas phase, for which the most frequently used functionals perform poorly. Experimental enthalpies of formation are used for the fragments for the isodesmic reactions, which provides the first coupling of experimental and theoretical data to create a unified thermochemistry database for adsorbates on Pt(111). Thermochemical data derived with this method deviates significantly from the adsorption reaction approach, and it creates an entirely new thermochemistry network for the adsorbates. The demonstrated concept provides a universally applicable framework with widespread application and a significant advancement in the determination of more accurate thermophysical properties of adsorbates.

Acknowledgement

BK acknowledges financial support from the Alexander von Humboldt Foundation through a Feodor Lynen scholarship for postdoctoral researchers. BK and CFG gratefully acknowledge support by the U.S. Department of Energy, Office of Science, Basic Energy Sciences, under Award #0000232253 and #DE-SC0019441, as part of the Computational Chemical Sciences Program. We thank Gabriel Gusmão, Andrew J. Medford, Andrew A. Peterson, Zachary W. Ulissi, and Charlie T. Campbell for helpful discussions on the thermochemistry of adsorbates, and we thank Sarah Elliott and Stephen Klippenstein for help with the iodomethane thermochemistry.

Supporting Information Available

Supporting information to this article is available online.

Detailed information on the CBH method; DFT raw data; derivations for the experimental enthalpies of formation; CBH reactions for all adsorbates.

References

(1) Wehinger, G. D.; Ambrosetti, M.; Cheula, R.; Ding, Z.-B.; Isoz, M.; Kreitz, B.; Kuhlmann, K.; Kutscherauer, M.; Niyogi, K.; Poissonnier, J.; Réocreux, R.; Rudolf, D.; Wagner, J.; Zimmermann, R.; Bracconi, M.; Freund, H.; Krewer, U.; Maestri, M. Quo vadis multiscale modeling in reaction engineering? – A perspective. *Chem. Eng. Res. Des.* **2022**, *184*, 39–58.

(2) Pio, G.; Dong, X.; Salzano, E.; Green, W. H. Automatically generated model for light alkene combustion. *Combust. Flame* **2022**, *241*, 112080.

(3) Kreitz, B.; Lott, P.; Bae, J.; Blöndal, K.; Angeli, S.; Ulissi, Z. W.; Studt, F.; Goldsmith, C. F.; Deutschmann, O. Detailed Microkinetics for the Oxidation of Exhaust Gas Emissions through Automated Mechanism Generation. *ACS Catal.* **2022**, *12*, 11137–11151.

(4) Kreitz, B.; Sargsyan, K.; Blöndal, K.; Mazeau, E. J.; West, R. H.; Wehinger, G. D.; Turek, T.; Goldsmith, C. F. Quantifying the Impact of Parametric Uncertainty on Automatic Mechanism Generation for CO_2 Hydrogenation on Ni(111). *JACS Au* **2021**, *1*, 1656–1673.

(5) Sprowl, L. H.; Campbell, C. T.; Árnadóttir, L. Hindered Translator and Hindered Rotor Models for Adsorbates: Partition Functions and Entropies. *J. Phys. Chem. C* **2016**, *120*, 9719–9731.

(6) Blöndal, K.; Sargsyan, K.; Bross, D. H.; Ruscic, B.; Goldsmith, C. F. Adsorbate Partition Functions via Phase Space Integration: Quantifying the Effect of Translational Anharmonicity on Thermodynamic Properties. *J. Phys. Chem. C* **2021**, *125*, 20249–20260.

(7) Campbell, C. T. Energies of Adsorbed Catalytic Intermediates on Transition Metal Surfaces: Calorimetric Measurements and Benchmarks for Theory. *Acc. Chem. Res.* **2019**, *52*, 984–993.

(8) Silbaugh, T. L.; Campbell, C. T. Energies of Formation Reactions Measured for Adsorbates on Late Transition Metal Surfaces. *J. Phys. Chem. C* **2016**, *120*, 25161–25172.

(9) Wellendorff, J.; Silbaugh, T. L.; Garcia-Pintos, D.; Nørskov, J. K.; Bligaard, T.; Studt, F.; Campbell, C. T. A Benchmark Database for Adsorption Bond Energies to Transition Metal Surfaces and Comparison to Selected DFT Functionals. *Surf. Sci.* **2015**, *640*, 36–44.

(10) Benson, S. W.; Cruickshank, F. R.; Golden, D. M.; Haugen, G. R.; O'Neal, H. E.; Rodgers, A. S.; Shaw, R.; Walsh, R. Additivity Rules for the Estimation of Thermochemical Properties. *Chem. Rev.* **1969**, *69*, 279–324.

(11) Salciccioli, M.; Chen, Y.; Vlachos, D. G. Density Functional Theory-Derived Group Additivity and Linear Scaling Methods for Prediction of Oxygenate Stability on Metal Catalysts: Adsorption of Open-Ring Alcohol and Polyol Dehydrogenation Intermediates on Pt-Based Metals. *J. Phys. Chem. C* **2010**, *114*, 20155–20166.

(12) Wittreich, G. R.; Vlachos, D. G. Python Group Additivity (pGrAdd) Software for Estimating Species Thermochemical Properties. *Comput. Phys. Commun.* **2022**, *273*, 108277.

(13) Chen, B. W. J.; Xu, L.; Mavrikakis, M. Computational Methods in Heterogeneous Catalysis. *Chem. Rev.* **2021**, *121*, 1007–1048.

(14) Ruscic, B.; Bross, D. H. Active Thermochemical Tables (ATcT) Values Based on ver. 1.124 of the Thermochemical Network. `https://atct.anl.gov`, (accessed 2022-09-22).

(15) Ruscic, B.; Pinzon, R. E.; Morton, M. L.; von Laszevski, G.; Bittner, S. J.; Nijsure, S. G.; Amin, K. A.; Minkoff, M.; Wagner, A. F. Introduction to Active Thermochemical Tables: Several "Key" Enthalpies of Formation Revisited. *J. Phys. Chem. A* **2004**, *108*, 9979–9997.

(16) Klippenstein, S. J.; Harding, L. B.; Ruscic, B. Ab Initio Computations and Active Thermochemical Tables Hand in Hand: Heats of Formation of Core Combustion Species. *J. Phys. Chem. A* **2017**, *121*, 6580–6602.

(17) Peterson, K. A.; Feller, D.; Dixon, D. A. Chemical Accuracy in Ab Initio Thermochemistry and Spectroscopy: Current Strategies and Future Challenges. *Theor. Chem. Acc.* **2012**, *131*, 1079.

(18) Karton, A.; Rabinovich, E.; Martin, J. M. L.; Ruscic, B. W4 Theory for Computational Thermochemistry: In Pursuit of Confident Sub-kJ/Mol Predictions. *J. Chem. Phys.* **2006**, *125*, 144108.

(19) Harding, M. E.; Vázquez, J.; Ruscic, B.; Wilson, A. K.; Gauss, J.; Stanton, J. F. High-Accuracy Extrapolated *Ab Initio* Thermochemistry. III. Additional Improvements and Overview. *J. Chem. Phys.* **2008**, *128*, 114111.

(20) Jaeger, H. M.; Schaefer, H. F.; Demaison, J.; Császár, A. G.; Allen, W. D. Lowest-Lying Conformers of Alanine: Pushing Theory to Ascertain Precise Energetics and Semiexperimental R_e Structures. *J. Chem. Theory Comput.* **2010**, *6*, 3066–3078.

(21) Yang, N.; Medford, A. J.; Liu, X.; Studt, F.; Bligaard, T.; Bent, S. F.; Nørskov, J. K. Intrinsic Selectivity and Structure Sensitivity of Rhodium Catalysts for C_{2+} Oxygenate Production. *J. Am. Chem. Soc.* **2016**, *138*, 3705–3714.

(22) Foppa, L.; Margossian, T.; Kim, S. M.; Müller, C.; Copéret, C.; Larmier, K.; Comas-Vives, A. Contrasting the Role of Ni/Al_2O_3 Interfaces in Water-Gas Shift and Dry Reforming of Methane. *J. Am. Chem. Soc.* **2017**, *139*, 17128–17139.

(23) Matera, S.; Schneider, W. F.; Heyden, A.; Savara, A. Progress in Accurate Chemical Kinetic Modeling, Simulations, and Parameter Estimation for Heterogeneous Catalysis. *ACS Catal.* **2019**, *9*, 6624–6647.

(24) Gürbüz, E. I.; Hibbitts, D. D.; Iglesia, E. Kinetic and Mechanistic Assessment of Alkanol/Alkanal Decarbonylation and Deoxygenation Pathways on Metal Catalysts. *J. Am. Chem. Soc.* **2015**, *137*, 11984–11995.

(25) Kreitz, B.; Wehinger, G. D.; Goldsmith, C. F.; Turek, T. Microkinetic Modeling of the Transient CO_2 Methanation with DFT-Based Uncertainties in a Berty Reactor. *ChemCatChem* **2022**, e202200570.

(26) Kreitz, B.; Wehinger, G. D.; Goldsmith, C. F.; Turek, T. Microkinetic Modeling of the CO_2 Desorption from Supported Multifaceted Ni Catalysts. *J. Phys. Chem. C* **2021**, *125*, 2984–3000.

(27) Sutton, J. E.; Guo, W.; Katsoulakis, M. A.; Vlachos, D. G. Effects of Correlated Parameters and Uncertainty in Electronic-Structure-Based Chemical Kinetic Modelling. *Nat. Chem.* **2016**, *8*, 331–337.

(28) Pople, J. A.; Radom, L.; Hehre, W. J. Molecular Orbital Theory of the Electronic Structure of Organic Compounds. VII. Systematic Study of Energies, Conformations, and Bond Interactions. *J. Am. Chem. Soc.* **1971**, *93*, 289–300.

(29) Hehre, W. J.; Ditchfield, R.; Radom, L.; Pople, J. A. Molecular Orbital Theory of the Electronic Structure of Organic Compounds. V. Molecular Theory of Bond Separation. *J. Am. Chem. Soc.* **1970**, *92*, 4796–4801.

(30) Wheeler, S. E.; Houk, K. N.; Schleyer, P. v. R.; Allen, W. D. A Hierarchy of Homodesmotic Reactions for Thermochemistry. *J. Am. Chem. Soc.* **2009**, *131*, 2547–2560.

(31) Ramabhadran, R. O.; Raghavachari, K. The Successful Merger of Theoretical Thermochemistry with Fragment-Based Methods in Quantum Chemistry. *Acc. Chem. Res.* **2014**, *47*, 3596–3604.

(32) Wheeler, S. E. Homodesmotic Reactions for Thermochemistry: Homodesmotic Reactions for Thermochemistry. *WIREs Comput. Mol. Sci.* **2012**, *2*, 204–220.

(33) Ramabhadran, R. O.; Raghavachari, K. Theoretical Thermochemistry for Organic Molecules: Development of the Generalized Connectivity-Based Hierarchy. *J. Chem. Theory Comput.* **2011**, *7*, 2094–2103.

(34) Sengupta, A.; Raghavachari, K. Prediction of Accurate Thermochemistry of Medium and Large Sized Radicals Using Connectivity-Based Hierarchy (CBH). *J. Chem. Theory Comput.* **2014**, *10*, 4342–4350.

(35) Sengupta, A.; Ramabhadran, R. O.; Raghavachari, K. Accurate and Computationally Efficient Prediction of Thermochemical Properties of Biomolecules Using the Generalized Connectivity-Based Hierarchy. *J. Phys. Chem. B* **2014**, *118*, 9631–9643.

(36) Xu, H.; Xu, Z.; Liu, L.; Li, Z.; Zhu, Q.; Ren, H. Method and Automatic Program for Accurate Thermodynamic Data of Reaction Mechanisms for Combustion Modeling. *Fuel* **2022**, *329*, 125431.

(37) Mulvihill, C. R.; Danilack, A. D.; Goldsmith, C. F.; Demireva, M.; Sheps, L.; Georgievskii, Y.; Elliott, S. N.; Klippenstein, S. J. Non-Boltzmann Effects in Chain Branching and Pathway Branching for Diethyl Ether Oxidation. *Energy Fuels* **2021**, *35*, 17890–17908.

(38) Almeida, M. O.; Kolb, M. J.; Lanza, M. R. V.; Illas, F.; Calle-Vallejo, F. Gas-Phase Errors Affect DFT-Based Electrocatalysis Models of Oxygen Reduction to Hydrogen Peroxide. *ChemElectroChem* **2022**, *9*.

(39) Peterson, A. A.; Abild-Pedersen, F.; Studt, F.; Rossmeisl, J.; Nørskov, J. K. How Copper Catalyzes the Electroreduction of Carbon Dioxide into Hydrocarbon Fuels. *Energy & Environmental Science* **2010**, *3*, 1311.

(40) Blondal, K.; Jelic, J.; Mazeau, E.; Studt, F.; West, R. H.; Goldsmith, C. F. Computer-Generated Kinetics for Coupled Heterogeneous/Homogeneous Systems: A Case Study in Catalytic Combustion of Methane on Platinum. *Ind. Eng. Chem. Res.* **2019**, *58*, 17682–17691.

(41) Liu, M.; Grinberg Dana, A.; Johnson, M. S.; Goldman, M. J.; Jocher, A.; Payne, A. M.; Grambow, C. A.; Han, K.; Yee, N. W.; Mazeau, E. J.; Blondal, K.; West, R. H.; Goldsmith, C. F.; Green, W. H. Reaction Mechanism Generator v3.0: Advances in Automatic Mechanism Generation. *J. Chem. Inf. Model.* **2021**, *61*, 2686–2696.

(42) Goldsmith, C. F.; West, R. H. Automatic Generation of Microkinetic Mechanisms for Heterogeneous Catalysis. *J. Phys. Chem. C* **2017**, *121*, 9970–9981.

(43) Johnson, M. S.; Dong, X.; Grinberg Dana, A.; Chung, Y.; Farina, D.; Gillis, R. J.; Liu, M.; Yee, N. W.; Blondal, K.; Mazeau, E.; Grambow, C. A.; Payne, A. M.; Spiekermann, K. A.; Pang, H.-W.; Goldsmith, C. F.; West, R. H.; Green, W. H. RMG Database for Chemical Property Prediction. *J. Chem. Inf. Model.* **2022**, *62*, 4906–4915.

(44) Giannozzi, P.; Baroni, S.; Bonini, N.; Calandra, M.; Car, R.; Cavazzoni, C.; Ceresoli, D.; Chiarotti, G. L.; Cococcioni, M.; Dabo, I.; Dal Corso, A.; de Gironcoli, S.; Fabris, S.; Fratesi, G.; Gebauer, R.; Gerstmann, U.; Gougoussis, C.; Kokalj, A.; Lazzeri, M.; Martin-Samos, L.; Marzari, N.; Mauri, F.; Mazzarello, R.; Paolini, S.; Pasquarello, A.; Paulatto, L.; Sbraccia, C.; Scandolo, S.; Sclauzero, G.; Seitsonen, A. P.; Smogunov, A.; Umari, P.; Wentzcovitch, R. M. QUANTUM ESPRESSO: a modular and open-source software project for quantum simulations of materials. *J. Phys.: Condens. Matter* **2009**, *21*, 395502.

(45) Giannozzi, P.; Andreussi, O.; Brumme, T.; Bunau, O.; Buongiorno Nardelli, M.; Calandra, M.; Car, R.; Cavazzoni, C.; Ceresoli, D.; Cococcioni, M.; Colonna, N.; Carnimeo, I.; Dal Corso, A.; de Gironcoli, S.; Delugas, P.; DiStasio, R. A.; Ferretti, A.; Floris, A.; Fratesi, G.; Fugallo, G.; Gebauer, R.; Gerstmann, U.; Giustino, F.; Gorni, T.; Jia, J.; Kawamura, M.; Ko, H.-Y.; Kokalj, A.; Küçükbenli, E.; Lazzeri, M.; Marsili, M.; Marzari, N.; Mauri, F.; Nguyen, N. L.; Nguyen, H.-V.; Otero-de-la Roza, A.; Paulatto, L.; Poncé, S.; Rocca, D.; Sabatini, R.; Santra, B.; Schlipf, M.; Seitsonen, A. P.; Smogunov, A.; Timrov, I.; Thonhauser, T.; Umari, P.; Vast, N.; Wu, X.; Baroni, S. Advanced capabilities for materials modelling with Quantum ESPRESSO. *J. Phys.: Condens. Matter* **2017**, *29*, 465901.

(46) Wellendorff, J.; Lundgaard, K. T.; Møgelhøj, A.; Petzold, V.; Landis, D. D.; Nørskov, J. K.; Bligaard, T.; Jacobsen, K. W. Density Functionals for Surface Science: Exchange-correlation Model Development with Bayesian Error Estimation. *Phys. Rev. B* **2012**, *85*, 235149.

(47) Streibel, V.; Aljama, H. A.; Yang, A.-C.; Choksi, T. S.; Sánchez-Carrera, R. S.; Schäfer, A.; Li, Y.; Cargnello, M.; Abild-Pedersen, F. Microkinetic Modeling of Propene Combustion on a Stepped, Metallic Palladium Surface and the Importance of Oxygen Coverage. *ACS Catal.* **2022**, *12*, 1742–1757.

(48) Abbas, N. M.; Madix, R. J. The Effects of Structured Overlayers of Sulfur on the Kinetics and Mechanism of Simple Reactions on Pt(111): I. Formaldehyde Decomposition. *Appl. Surf. Sci.* **1981**, *7*, 241–275.

(49) Windham, R. G.; Bartram, M. E.; Koel, B. E. Coadsorption of Ethylene and Potassium on Platinum (111). 1. Formation of a π-Bonded State of Ethylene. *J. Phys. Chem.* **1988**, *92*, 2862–2870.

(50) Karp, E. M.; Campbell, C. T.; Studt, F.; Abild-Pedersen, F.; Nørskov, J. K. Energetics of Oxygen Adatoms, Hydroxyl Species and Water Dissociation on Pt(111). *J. Phys. Chem. C* **2012**, *116*, 25772–25776.

(51) Karp, E. M.; Silbaugh, T. L.; Campbell, C. T. Energetics of Adsorbed CH_3 on Pt(111) by Calorimetry. *J. Am. Chem. Soc.* **2013**, *135*, 5208–5211.

(52) Karp, E. M.; Silbaugh, T. L.; Crowe, M. C.; Campbell, C. T. Energetics of Adsorbed Methanol and Methoxy on Pt(111) by Microcalorimetry. *J. Am. Chem. Soc.* **2012**, *134*, 20388–20395.

(53) Kreitz, B.; Abeywardane, K.; Goldsmith, C. F. Data for Linking Experimental and Ab-initio Thermochemistry of Adsorbates with a Generalized Thermochemical Hierarchy. 2023; `https://doi.org/10.5281/zenodo.7506509`.

(54) Wolcott, C. A.; Green, I. X.; Silbaugh, T. L.; Xu, Y.; Campbell, C. T. Energetics of Adsorbed CH_2 and CH on Pt(111) by Calorimetry: The Dissociative Adsorption of Diiodomethane. *J. Phys. Chem. C* **2014**, *118*, 29310–29321.

(55) Kubota, J.; Ichihara, S.; Kondo, J. N.; Domen, K.; Hirose, C. π-Bonded Ethene on Pt(111) Surface Studied by IRAS. *Surf. Sci.* **1996**, *357-358*, 634–638.

(56) Papp, C.; Fuhrmann, T.; Tränkenschuh, B.; Denecke, R.; Steinrück, H.-P. Kinetic Isotope Effects and Reaction Intermediates in the Decomposition of Methyl on Flat and Stepped Platinum (111) Surfaces. *Chem. Phys. Lett.* **2007**, *442*, 176–181.

(57) Kreitz, B.; Wehinger, G. D.; Goldsmith, C. F.; Turek, T. In *30th European Symposium on Computer Aided Process Engineering*; Pierucci, S., Manenti, F., Bozzano, G. L., Manca, D., Eds.; Comput.-Aided Chem. Eng.; Elsevier, 2020; Vol. 48; pp 529–534.

(58) Mazeau, E. J.; Satpute, P.; Blöndal, K.; Goldsmith, C. F.; West, R. H. Automated Mechanism Generation Using Linear Scaling Relationships and Sensitivity Analyses Applied to Catalytic Partial Oxidation of Methane. *ACS Catal.* **2021**, *11*, 7114–7125.

(59) Wehinger, G. D.; Kreitz, B.; Goldsmith, C. F. Non-Idealities in Lab-Scale Kinetic Testing: A Theoretical Study of a Modular Temkin Reactor. *Catalysts* **2022**, *12*, 349.

(60) Christensen, R.; Hansen, H. A.; Vegge, T. Identifying Systematic DFT Errors in Catalytic Reactions. *Catal. Sci. Technol.* **2015**, *5*, 4946–4949.

(61) Silbaugh, T. L.; Karp, E. M.; Campbell, C. T. Energetics of Methanol and Formic Acid Oxidation on Pt(111): Mechanistic Insights from Adsorption Calorimetry. *Surf. Sci.* **2016**, *650*, 140–143.

(62) Saerens, S.; Sabbe, M. K.; Galvita, V. V.; Redekop, E. A.; Reyniers, M.-F.; Marin, G. B. The Positive Role of Hydrogen on the Dehydrogenation of Propane on Pt(111). *ACS Catal.* **2017**, *7*, 7495–7508.

(63) Cushing, G. W.; Navin, J. K.; Donald, S. B.; Valadez, L.; Johánek, V.; Harrison, I. C-H Bond Activation of Light Alkanes on Pt(111): Dissociative Sticking Coefficients, Evans-Polanyi Relation, and Gas-Surface Energy Transfer. *J. Phys. Chem. C* **2010**, *114*, 17222–17232.

(64) Segner, J.; Campbell, C.; Doyen, G.; Ertl, G. Catalytic oxidation of CO on Pt(111): The influence of surface defects and composition on the reaction dynamics. *Surf. Sci.* **1984**, *138*, 505–523.

(65) Brown, W. A.; Kose, R.; King, D. A. Femtomole Adsorption Calorimetry on Single-Crystal Surfaces. *Chem. Rev.* **1998**, *98*, 797–832.

(66) Yeo, Y.; Stuck, A.; Wartnaby, C.; King, D. Microcalorimetric Study of Ethylene Adsorption on the Pt{111} Surface. *Chem. Phys. Lett.* **1996**, *259*, 28–36.

(67) Iyer, G. R.; Rubenstein, B. M. Finite-Size Error Cancellation in Diffusion Monte Carlo Calculations of Surface Chemistry. *J. Phys. Chem. A* **2022**, *126*, 4636–4646.

(68) Sauer, J. Ab Initio Calculations for Molecule-Surface Interactions with Chemical Accuracy. *Acc. Chem. Res.* **2019**, *52*, 3502–3510.

(69) Sheldon, C.; Paier, J.; Sauer, J. Adsorption of CH $_4$ on the Pt(111) Surface: Random Phase Approximation Compared to Density Functional Theory. *J. Chem. Phys.* **2021**, *155*, 174702.

(70) Ghosh, M. K.; Elliott, S. N.; Somers, K. P.; Klippenstein, S. J.; Curran, H. J. Group Additivity Values for the Heat of Formation of C2–C8 Alkanes, Alkyl Hydroperoxides, and Their Radicals. *Combust. Flame* **2022**, 112492.